Short communication

Cu$_5$Si–Si/C composites for lithium-ion battery anodes

Yanna NuLi, Baofeng Wang, Jun Yang *, Xianxia Yuan, Zifeng Ma

Department of Chemical Engineering, Shanghai Jiao Tong University, Shanghai 200240, PR China

Available online 27 June 2005

Abstract

Cu$_5$Si–Si/C composites with precursor atomic ratio of Si:Cu = 1, 2 and 4.5 have been produced by high-energy ball-milling of a mixture of copper–silicon alloy and graphite powder for anode materials of lithium-ion battery. X-ray diffraction and scanning electron microscope measurements show that Cu$_5$Si alloy is formed after the intensive ball milling and alloy particles along with low-crystallite Si are interspersed in graphite uniformly. Cu$_5$Si–Si/C composite electrodes deliver a larger reversible capacity than commercialized graphite and better cyclability than silicon. The increase of copper amount in the composites decreases reversible capacity but improves cycling performance. Cu$_5$Si–Si/C composite with Si:Cu = 1 demonstrates an initial reversible capacity of 612 mAh g^{-1} at 0.2 mA cm^{-2} in the voltage range from 0.02 to 1.5 V. The capacity retention is respectively 74.5 and 70.0% at the 40th cycle at the current density of 0.2 and 1 mA cm^{-2}.
© 2005 Elsevier B.V. All rights reserved.

Keywords: Cu$_5$Si–Si/C composites; Ball-milling; Lithium-ion batteries; Anode; Electrochemical characterization

1. Introduction

Graphite is commonly used as an anode material in lithium batteries, but higher capacity alternatives such as Al, Si, Sn and Sb that could alloy lithium, have been investigated as possible replacements for graphite. Especially, silicon is the most attractive due to as high as 4000 mAh g^{-1} theoretical capacity for the reaction of silicon and lithium to maximum uptake of Li$_{21}$Si$_5$ [1,2]. The major hindrance to its application is the poor cyclability caused by mechanical cracking due to the volume change of lithium silicide during charge–discharge process and high irreversible capacity at the first cycle resulted from phase transformation, dangling bond as well as electronic contact loss by the volume change [3]. To overcome these problems, numerous studies have been devoted to the synthesis of Si/C composites with highly dispersed particles to minimize the mechanical stress related to lithium insertion and extraction [4–6]. Another effective approach was synthesizing metal silicide alloys with less active or inactive metal elements and active Si such as Fe–Si [7], Co–Si [8], Ni–Si [9], Cr–Si [10], Ca–Si [11] and Mg–Si [12] etc. The ductile inactive matrix simul-taneously generated during lithium insertion, which buffers the volume change of lithium silicide.

Mechanical milling/alloying has been shown to be a powerful technique to produce alloy powders with a homogeneous structure [13]. In this work, Cu$_5$Si–Si with different precursor atomic ratio of Si:Cu are dispersed in graphite, which provides not only mechanical and conductivity support for the dispersed phase but also possesses electrochemical reactivity towards lithium. The objective of this investigation is to utilize the high conductivity of inert copper and low volume effect of graphite to improve the cyclability of silicon active material.

2. Experimental

2.1. Material preparation

The ball-milling was carried out in a planetary ball mill (Fritsch P-6 Planetary Mono Mill). Two grams of powder mixtures of pure Cu (99.7% pure) and Si (<1 μm, 99% up pure) powders with different atomic ratios of Si:Cu = 1, 2, 4.5 and 10 stainless steel grinding balls were placed in a 80 ml stainless steel grinding bowl in an argon-filled glove box to prepare Cu$_5$Si–Si. Milling was performed at a rotation rate of

* Corresponding author. Tel.: +86 21 5474 7667; fax: +86 21 5474 1297.
  E-mail address: yangj723@sjtu.edu.cn (J. Yang).

400 rpm for 7 h. Annealed samples were prepared by heating the Cu_5Si–Si mixture at 600 °C for 4h under a flow of argon and then ball-milling at 300 rpm for 60 min. Cu_5Si–Si/C composites (60 wt.% Cu_5Si–Si + 40 wt.% graphite) were fabricated by the high energy milling of as-formed Cu_5Si–Si and graphite powder (1–2 μm, Aldrich) at a rotation rate of 450 rpm for 20 min. The Si/C and ball-milled Si/C samples with 60:40 wt.% were fabricated by milling of graphite and Si, or previously milled Si powder at 450 rpm for 20 min, respectively. Previously milled Si was obtained by milling Si powder at 400 rpm for 7 h. The powders produced were characterized by XRD using Philips 3100E diffractometer with Cu Kα radiation. The morphology and microstructure of ball-milled powders were observed with a scanning electron microscopy (Hitachi S 2150).

2.2. Cells assembling and electrochemical test

Electrodes were prepared by drying slurry (86 wt.% active material, 6 wt.% acetylene black and 8 wt.% polyvinylidene fluoride dissolved in *N*-methyl-2-pyrrolidine for samples without graphite, and 90:0:10 wt.% for samples containing graphite) coated on a copper foil at 130 °C under vacuum. Electrode disks (ϕ 1.4 cm) were punched from the foil and weighed. Electrochemical behavior of the test materials was examined via CR2025 coin cells with lithium metal counter electrode, Celgard 2700 membrane separator, and electrolyte of 1 M $LiPF_6$ dissolved in a mixture of ethyl carbonate (EC) and dimethyl carbonate (DMC) (1:1 in weight ratio). The cells were assembled in an argon-filled glove box containing less than 1 ppm each of oxygen and moisture.

Discharge–charge measurements of the coin cells were carried out at current densities of 0.2 and 1 mA cm^{-2} with voltage cut-off of 0.02/1.5 V versus Li/Li$^+$. Cyclic voltammograms (CVs) were obtained using CHI750A electrochemical workstation.

3. Results and discussion

The XRD patterns of Cu_5Si–Si/C composites with different precursor atomic ratio of Si:Cu are shown in Fig. 1. For comparison, the XRD patterns of Si/C and ball-milled Si/C powders obtained by milling Si and graphite at 450 rpm for 20 min are also shown (pretreatment of silicon: non-milled in Fig. 1a, ball-milled for 7 h in Fig. 1b). As shown in Fig. 1a, the diffraction peaks at $2\theta = 28.4°$, 47.3°, 56.1°, 69.1°, 76.4° and 88.0° can be attributed to (1 1 1), (2 2 0), (3 1 1), (4 0 0), (3 3 1) and (4 2 2) reflections of Si (JCPDS file 27–1402). The diffraction peaks at $2\theta = 26.4°$, 54.5° and 77.4° correspond to (0 0 2), (0 0 4) and (1 1 0) diffraction intensity of graphite (JCPDS file 41–1487), and the broad hump at 45° indicates that part of graphite is amorphized, as shown in Fig. 1b. Peak broadening of Si is related to milling-induced crystallite size reduction. A mixture of Cu_5Si and Si is detected instead of a pure alloy for three composite samples, as shown
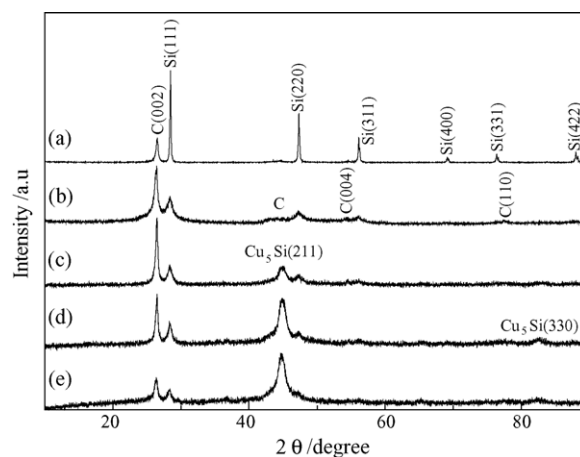

Fig. 1. The XRD patterns for (a) Si/C, (b) ball-milled Si/C, (c) (d) and (e) Cu_5Si–Si/C composites with different precursor atomic ratio of Si:Cu = 4.5, 2 and 1, respectively.

in Fig. 1c–e. The diffraction peaks at $2\theta = 44.6°$ and 82.4° can be attributed to (2 1 1) and (3 3 0) reflections of Cu_5Si (JCPDS file 04–0841) and the diffraction intensity was influenced by the content of Cu in the composites. With increase of the Cu content, the XRD intensity of Cu_5Si increases and crystallization of graphite and silicon tends to decline.

Scanning electron micrographs of ball-milled Cu_5Si–Si/C (Si:Cu = 1) and Si/C composites are given in Fig. 2a and b, respectively. In the case of Cu_5Si–Si/C powder, fine silicon particles probably are pinned in inactive Cu_5Si alloy phase via the good ductibility and affinity to Si of Cu_5Si. All the components tend to form large agglomerates, obviously different from the morphology of ball-milled Si/C, in which many small silicon particles separately coexist with much larger particles with sizes of tens of microns. It is apparent that silicon is better incorporated with the rest components in Cu_5Si–Si/C than in Si/C composite.

Preliminary cycle life studies at 0.2 mA cm^{-2} for Cu_5Si–Si and Cu_5Si–Si/C composite anode materials are shown in Fig. 3. The capacity decreases drastically in the second cycle for all the samples and the first cycle efficiency is about 60–70%. Addition of copper and the increase in the Cu content improves the cycling stability at the expense of the reversible capacity. This improvement could be attributed to high dispersion and fixation of active Si domains in conductive Cu_5Si matrix. However, even for Cu_5Si–Si composite with Si:Cu = 1 the capacity fade in the initial cycles remains serious. Heat treatment at 600 °C for 4 h was attempted to enhance its cyclability, but annealed sample shows much lower capacity probably due to deactivation of more active-silicon by alloying with copper and coating with inert Cu_5Si alloy. A further improvement in the electrochemical performance can be achieved by incorporation of graphite, a good mixed-conductor with small volume expansion by Li-intercalation. This is because the flexible graphite buffers the volume change of silicon active material and reduces mechanical stress within the electrode. Cu_5Si–Si/C composite
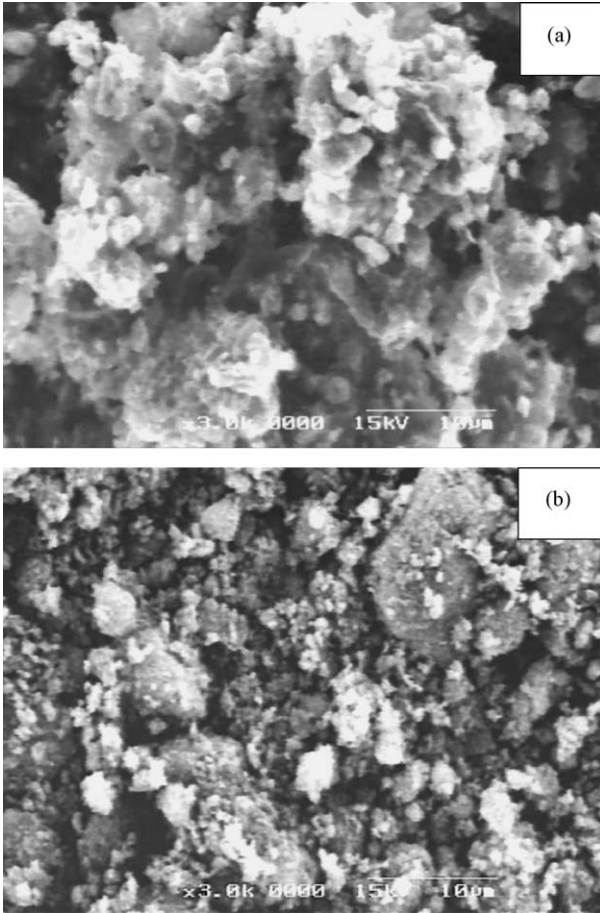
Fig. 2. SEM image of (a) Cu_5Si–Si/C composite with Si:Cu = 1, (b) ball-milled Si/C.

materials combine high lithium storage capacity of silicon with good cyclability of graphite. Comparing with rapid decay of cycle performance of the ball-milled Si/C anode, the capacity turns to be stable after the second cycle for Cu_5Si–Si/C sample with Si:Cu = 1, and the electrode provides an initial reversible capacity of 612 mAh g^{-1} and around
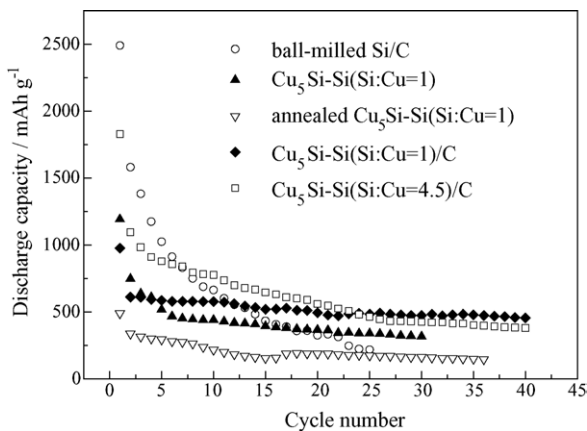

Fig. 3. Cycle performance of ball-milled Si/C, Cu_5Si–Si, annealed Cu_5Si–Si and Cu_5Si–Si/C with different precursor atomic ratio of Si:Cu at 0.2 mA cm^{-2}.
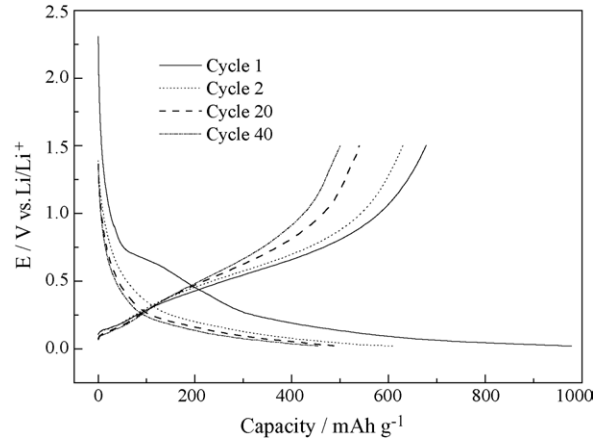

Fig. 4. Discharge and charge profiles for Cu_5Si–Si/C composite electrode with Si:Cu = 1 at 0.2 mA cm^{-2}.

74.5% of reversible capacity can be retained at the 40th cycle at 0.2 mA cm^{-2}. Moreover, it is noted that addition of copper can not only enhance the cyclability, but also improve the kinetic behavior by means of enhanced dispersion and conductivity of active silicon domains. When current density is increased from 0.2 to 1 mA cm^{-2}, 89.9% of the initial reversible capacity can be retained for Cu_5Si–Si/C composite with Si:Cu = 1, but only 51.2% for ball-milled Si/C sample.

Fig. 4 presents a discharge and charge profile of the Cu_5Si–Si/C composite anode with Si:Cu = 1 at 0.2 mA cm^{-2}. The voltage trend of the first discharge is obviously different from the following ones. A plateau at about 0.65 V can be observed in the first discharge, which disappears in the subsequent cycles. The SEI formation related to electrolyte decomposition may to be responsible for it. The subsequent curves demonstrate a smooth profile, indicating the low crystalline of the sample.

The cyclic voltammograms (CVs) of Si/C and Cu_5Si–Si/C with Si:Cu = 1 electrodes for the first five cycles at a scan rate of 0.1 mV s^{-1} are shown in Fig. 5a and b, respectively. Peak A at about 0.6 V in the first reduction process vanishes in the following cycles. This irreversible reaction is, in a great part, associated with SEI formation. It is noted that peak A almost does not exist for Si/C mixture milled for only 20 min (Fig. 5a). But ball-milling of Si–Cu mixture for 7 h greatly increases the specific surface area, which consumes more charge for SEI formation, leading to the formation of a big irreversible peak A (Fig. 5b). A similar result is also observed for ball-milled Si/C electrode (silicon was previously ball-milled for 7 h). Peaks B/B′ and B″ are attributed to the potential-dependent formation and disappearance of Li–Si alloys of different compositions [14]. For Cu_5Si–Si/C electrode, Peak B disappears and B′ and B″ amalgamate into one broad peak with some shifting, which may be related to the high amorphization extent of Si after milling. Peak C located at 0.26 V could be due to the deintercalation of Li$^+$ from graphite [15]. Compared to Si/C sample, Cu_5Si–Si/C composite electrode exhibits better cycle reproducibility.
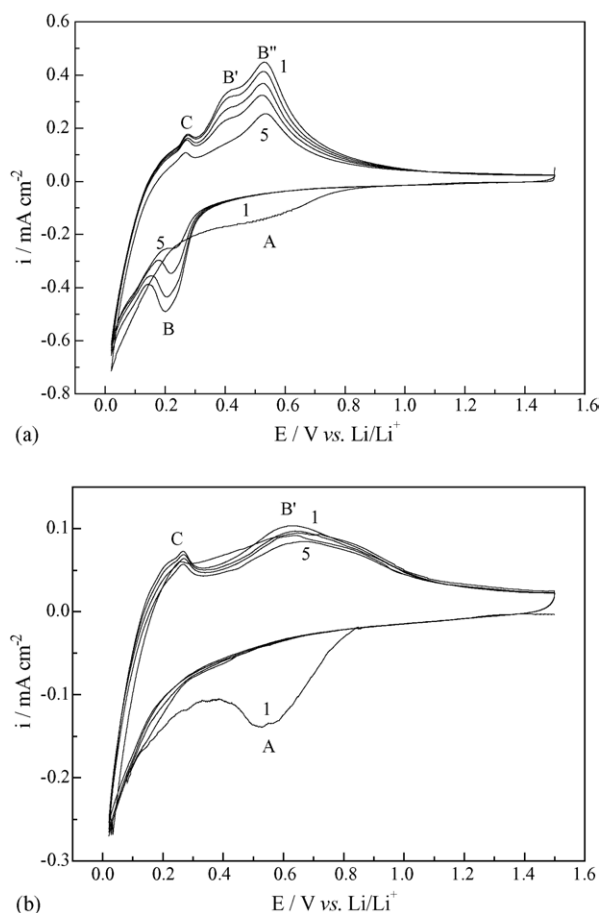
Fig. 5. Cyclic voltammograms of (a) Si/C and (b) Cu_5Si–Si/C with Si:Cu = 1 electrodes for the first five cycles at 0.1 mV s^{-1}.

4. Conclusions

Ball-milling of Cu and Si powders produces Cu_5Si alloy integrated with unalloyed silicon. Such a structure can endure volume change of active Si host for lithium insertion and extraction and improve the conductivity of silicon in the electrode. Electrochemical tests show the addition of copper improves the cycling stability at the expense of the reversible capacity. Heat treatment of the milled sample at 600 °C, how-ever, will cut the cycle capacity drastically probably due to deactivation of more active-silicon by alloying with copper and coating with inert Cu_5Si alloy. On the other hand, inter-spersing the Cu_5Si–Si powder in low volume-changed and flexible graphite can further enhance the electrode perfor-mance. Cu_5Si–Si/C composite anode material with Si:Cu = 1 provides an initial reversible capacity of 612 mAh g^{-1} and around 74.5% of reversible capacity can be retained at the 40th cycle at 0.2 mA cm^{-2}, against 14.1% at the 25th cycle for ball-milled Si/C electrode. For practical application, the initial irreversible capacity must be minimized.

References

[1] S. Lai, J. Electrochem. Soc. 123 (1976) 1196.
[2] R.A. Sharma, R.N. Seefurth, J. Electrochem. Soc. 123 (1976) 1763.
[3] Z.S. Wen, J. Yang, B.F. Wang, K. Wang, Y. Liu, Electochem. Com-mun. 5 (2003) 165.
[4] J. Yang, B.F. Wang, K. Wang, Y. Liu, J.Y. Xie, Z.S. Wen, Elec-trochem. Solid-State Lett. 6 (2003) 154.
[5] Weibing. Xing, A.M. Wilson, K. Eguchi, G. Zank, J.R. Dahn, J. Electrochem. Soc. 144 (1997) 2410.
[6] A.M. Wilson, J.R. Dahn, J. Electrochem. Soc. 142 (1995) 326.
[7] G.X. Wang, L. Sun, D.H. Bradhurst, S. Zhong, S.X. Dou, H.K. Liu, J. Power Sources 88 (2000) 278.
[8] A. Netz, R.A. Huggins, W. Weppner, J. Power Sources 119–121 (2003) 95.
[9] G.X. Wang, L. Sun, D.H. Bradhurst, S. Zhong, S.X. Dou, H.K. Liu, J. Alloys Compd. 306 (2000) 249.
[10] W.J. Weydanz, M. Wohlfahrt-Mehrens, R.A. Huggins, J. Power Sources 81–82 (1999) 237.
[11] J. Wolfenstine, J. Power Sources 124 (2003) 241.
[12] G.A. Roberts, E.J. Cairns, J.A. Reimer, J. Power Sources 110 (2002) 424.
[13] C.S. Wang, G.T. Wu, X.B. Zhang, Z.F. Qi, W.Z. Li, J. Electrochem. Soc. 145 (1998) 2751.
[14] C.J. Wen, R.A. Huggins, J. Solid State Chem. 37 (1981) 271.
[15] M.D. Levi, D. Aurbach, J. Electroanal. Chem. 421 (1997) 79.